International Journal of High Speed Electronics and Systems
Vol. 16, No. 1 (2006) 397–407

World Scientific
www.worldscientific.com

ELASTOMERIC INTERCONNECTS

Stéphanie P. Lacour, Joyelle Jones, Sigurd Wagner

Department of Electrical Engineering, Princeton University
*Princeton, New Jersey08544, USA**
slacour@princeton.edu

Teng Li, Z. Suo

Division of Engineering, Harvard University
Cambridge, Massachusetts 02138, USA

Received (5 February, 2005)
Revised (7 July, 2005)
Accepted (7 July, 2005)

Elastomeric interconnects made of patterned thin gold films on silicone membranes, can be reversibly bent, uniaxially or radially stretched while remaining electrically conducting. Such interconnects can be stretched to double their length, cycled 1,000 times without electrical failure. While the electrical resistance may increase threefold upon stretching, the resistance values still remain ~1,000 times below the typical input impedance of amorphous silicon thin film transistors. Therefore the stretchable gold films can function as interconnects for power and signal to a fully elastic thin film transistor inverter.

Keywords: thin metal film, silicone, elastic circuit.

1. Introduction

Beyond flexible displays[1,2] and RFID tags, conformable electronics have many other potential applications. Electronic circuits integrated on skin-like structures with large surface area will be able to recognize and respond to stimuli while being mechanically deformed (folded, deployed, stretched) or placed over randomly shaped objects. Applications include large area, foldable antennas, cockpit conformable display[3], conformable solar cells, smart sensor carpets, wearable sensor-arrays monitoring patient health and sensitive skin[4]. A whole new class of human-machine interfaces will be made possible. But designing, fabricating and evaluating stretchable electronic circuits is a challenge.

Our discovery of the stretchability of thin-film gold (Au) conductors on elastomeric substrate has enabled the development of a whole new type of electronic circuits. In this paper we present our approach to making and testing stretchable circuits based on soft

and elastic silicone substrates. We provide experimental details on the fabrication and patterning of elastomeric interconnects. We assess their electrical and mechanical characteristics for uni-axial and bi-axial stretching experiments. The electrical performance of an elastic thin-film transistor (TFT) inverter under mechanical stretching is presented. We conclude with perspective on elastic thin-film electronic circuits.

2. Elastic Electronic Circuits: Concept

2.1. *Architecture*

Today's microelectronic substrates and device materials have excellent electrical properties, but the mechanical failure of these stiff and brittle materials at small mechanical strain ($\varepsilon < 1\%$)[5] poses a significant challenge for the fabrication of conformable electronic circuits. To achieve large flexibility and stretchability, circuits may be prepared on soft and plastic substrates[6]. The skin-like structure is designed as a matrix of rigid subcircuit islands distributed on the soft substrate and interconnected with metallic conductors. Individual devices and subcircuits are patterned directly on the islands, which are made of a stiff material such as silicon nitride[6-7]. The circuits are completed with thin-film metal connecting the subcircuit islands. When the structure is deformed, the strain experienced by the islands is minimal, i.e., less than the fracture strain of device materials. Most of the mechanical deformation occurs in the part of the plastic substrate left uncovered by the islands. Interconnects must withstand this severe mechanical deformation, hence are a key component for stretchable electronic circuits.

2.2. *Stretchable metallization*

Our approach to stretchable metallization is to use a thin-film conductor compatible with microelectronics, i.e., evaporated gold. The film is deposited on an elastomeric membrane of polydimethylsiloxane (PDMS) that can be reversibly stretched and relaxed. To ensure its stretchability, the thin metal film can be prepared as an ordered wave that can be stretched flat without modifying the conductor structure, hence preserving its electrical conduction[8-10]. There are two ways to create a wavy conductor:

(i) metal deposition process on soft PDMS often generates a compressive stress in the plane of the metal film: the metal film spontaneously wrinkles[8,11]. When the metal is deposited in stripes of width < 1mm, ordered parallel waves may form in the film[8].

(ii) the PDMS membrane is pre-stretched prior to metal evaporation[9-10]. Upon release from pre-stretch, the PDMS substrate contracts in the X-direction (the conductor's length direction) and expands in the Y-direction due to the Poisson effect. The metal film comes under compressive stress in the X-direction, and forms a wave with vector in the X-direction[9].

Conductors prepared using either techniques are highly stretchable[8-9]. By mechanical modeling we are beginning to understand why the metal film when bonded to PDMS can be stretched far more than its freestanding counterpart[12-14]. Our model predicts that certain combinations of metal and substrate properties (thickness, hardness and Young's

moduli) indeed can be strained by up to 100% with the metal remaining continuous. A key requirement is that the metal does not detach from the substrate[12-14].
The interconnects we describe in this paper were prepared on relaxed PDMS membranes. Interconnects made on pre-stretched membranes were discussed in a previous article[9].

3. Interconnect Fabrication

3.1. *Materials*

The substrate is a 1mm thick PDMS membrane (Sylgard 184® from Dow Corning), compatible with microelectronic clean room equipment. Thin metal films, typically 25nm to 100nm thick gold on top of a 5nm thick chromium adhesion layer, are deposited by electron-beam evaporation directly on the bare PDMS surface. No PDMS surface treatment is performed before metal evaporations.
We chose gold as it is one of the most ductile metals with a high electrical conductivity. Two sample topographies are observed. The conductor surface can be wavy as shown in Figure 1a (built-in waves form during the deposition, the film remains bonded to the substrate). Occasionally we observe a flat surface (Figure 1b).

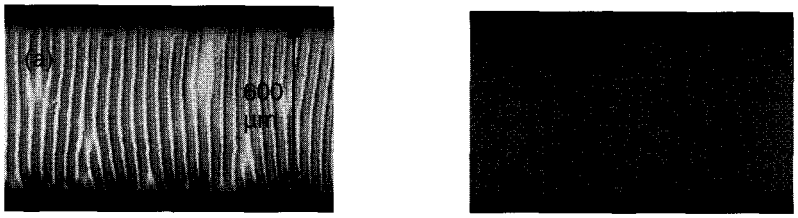

Figure 1. Optical micrographs[15] showing the topography of two gold conductors on 1mm thick initially relaxed PDMS membranes. (a) *Built-in waves* are observed in a 100nm thick, 600μm wide, 2.54 cm long gold conductor. The wavelength is ~25μm. (b) A 100nm thick, 200μm wide, 1.6cm long *flat* gold conductor.

3.2. *Patterning*

We have developed two techniques to pattern the Cr/Au metal films on PDMS. Standard photolithography cannot be readily used with silicone membranes. The silicone swells when exposed to organic solvents, and metal films peel. The two fabrication sequences and the resulting metal patterns are shown Figure 2(a) and (b).

3.2.1. *Kapton shadow masking*

We define conductor stripes by evaporating Cr and Au films through a shadow mask made of a 50μm thick polyimide foil (Fig. 2a). The mask is mounted directly on the PDMS surface prior to metal evaporation and is peeled off after metal deposition. This is a simple, dry patterning technique that can produce 200μm minimum feature size.

3.2.2. *Lift-off using Riston dry photo-resist*

Gold interconnects and contact pads are patterned on the PDMS by lift-off using Dupont Riston photo-resist. The UV-exposed and developed Riston film is laminated to the PDMS substrate prior to metal evaporation. Subsequently Cr and Au are electron-beam evaporated. The Riston film is then stripped in a KOH solution. This technique allows to pattern 100μm minimum feature size.

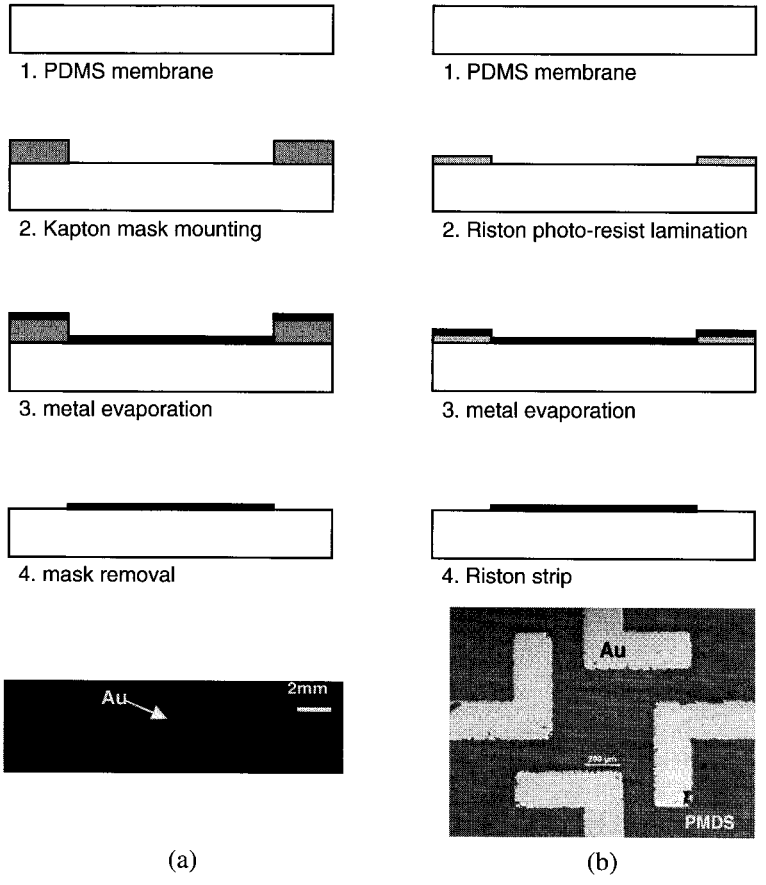

Figure 2. Two patterning techniques for elastomeric interconnects. (a) Kapton shadow masking; (b) Lift-off using Riston dry photoresist.

4. Electrical and mechanical properties

4.1. *Initial electrical resistance*

Typical metal stripes are 1.6cm to 5cm long and 0.1mm to 2.5mm wide. To evaluate their electrical resistance, electrical contacts are made using a non cured epoxy-based

silver paste. A 100μm dia. gold wire is embedded in the conductive paste and sandwiched between the substrate and another PDMS piece to ensure the electrical conduction as well as compliance.

The electrical resistance is measured with a Keithley 4210 source meter. The nominal resistivity is calculated as

$$\rho = R_{exp} \frac{W\ h}{L}. \quad (1)$$

where R_{exp} is the measured resistance, and L, W, and h are the macroscopic length, width, and thickness of the gold stripe, respectively. Reference samples prepared on glass slides have an electrical resistivity of ~ 5 $\mu\Omega$.cm, which is about twice that of bulk gold (2.3 $\mu\Omega$.cm[16]).

The electrical resistivity of wavy samples usually lies in the range of comparable samples on glass. The electrical resistivity of the flat conductors is higher, 3 to 100 times that of Au films on glass. Networks of micro-cracks distributed over the conductor surface are observed in the flat samples under the SEM[17]. We believe that the electrical path in these Au layers is tortuous and complex, as the film is a dense network of gold that surrounds randomly arranged voids thus increasing the apparent electrical resistivity of the film.

4.2. *1D and 2D stretching*

The metallic conductors can be bent[18] and uni-axially stretched[8-9,15]. Upon 1D uni-axial stretching, the sample is elongated along one direction (tensile strain, $\varepsilon_x>0$) and simultaneously contracted along the other two directions (compressive strain, $\varepsilon_y<0$, $\varepsilon_z<0$). Upon 2D radial stretching, the sample is stretched in all in-plane directions (tensile strain, $\varepsilon_r>0$, $\varepsilon_z<0$) and is compressed in the z (thickness) direction. From the equations of the sample's stretched area $A_{stretch}$ listed in Table 1, it is clear that for a given value of strain in one direction, 2D radial stretching produces larger changes in surface area, hence is more severe. The Poisson coefficient of an elastomer is 0.5.

Table 1. Surface area for 1D and 2D stretching

1D stretching	2D, biaxial, radial stretching
$A_{stretch} = (1+\varepsilon_x)(1-\upsilon\varepsilon_x)\times A_{init}$	$A_{stretch} = (1+\varepsilon_r)^2 \times A_{init}$
ε_x : applied strain, υ Poisson coefficient	ε_r : applied radial strain

We study 1D and 2D stretching with two different custom-made apparatuses.

4.2.1. *1D stretching*

In the uni-axial stretcher, the sample is mounted between two clamps as shown Figure 3a. a stepper motor controls the applied elongation. The left clamp (clamp 1) is stationary, while the right clamp (clamp 2) is translated away from clamp1, stretching the sample along its length. We record the electrical resistance with a Keithley 4140 source-meter. The surface topography is observed with a CCD camera microscope.

The applied tensile strain ε_x is defined by eq. (2):

$$\varepsilon_x = \frac{L_1 - L_0}{L_0} > 0. \quad (2)$$

with L_0 and L_1 the initial (relaxed) and stretched lengths of the stripe, respectively. Upon stretching , the tensile strain ε_x is accompanied by in-plane compressive strain ε_y defined as $\varepsilon_y = -\upsilon\varepsilon_x$ with υ the Poisson's coefficient of the elastomer ($\upsilon \sim 0.5$).

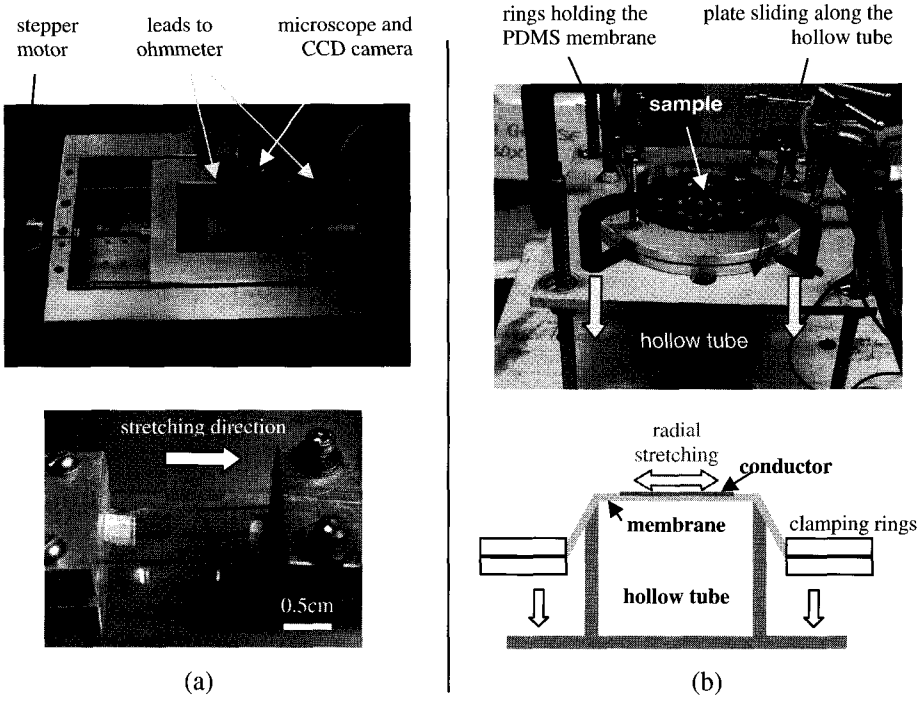

Figure 3. (a) 1D, uniaxial stretcher[8]. (top) Picture of the automated device. (bottom) zoom on one conductor held with the two clamps. (b) 2D, radial stretcher[19]. (top) Picture of the manual device; conductors on a silicone membrane are held in the clamping rings in the relaxed state $\varepsilon_r = 0\%$. The bright dots on the surface of the transparent substrate are electrical contacts made with silver paste. (bottom) Sketch of the device with a stretchable substrate under test.

4.2.2. *2D stretching*

For biaxial stretching, conductors are patterned on a circular membrane which is clamped at its rim. The membrane is stretched over the end of a hollow tube (Fig. 3b). The apparatus has three main parts: (i) a hollow tube of radius r, mounted vertically in the center of the apparatus, (ii) two aluminum rings between which the PDMS membrane is clamped and hold, (iii) an aluminum plate to which the rings are fixed by C-clamps, the plate can slide up and down around the tube. First the membrane is clamped between the rings and placed on top of the tube. When the plate is pulled down, the membrane is stretched in-plane, radially and uniformly over the edge of the hollow tube. The plate is

held at the desired position using a set of manually tightened nuts. The applied radial strain is defined by Eq. (3):

$$\varepsilon_r = \frac{(r+h)-(r+c)}{r+c}. \tag{3}$$

with r the tube radius, c the gap between the outside perimeter of the tube and the inside perimeter of the rings, and h the length of PDMS stretched between the tube and the rings.

4.2.3. *Electrical resistance under mechanical deformation*

Figure 4 presents the electrical resistance of 25nm thick elastomeric interconnects when uni-axially and radially stretched. The 1D stretched sample (sample 1) was 200μm wide and 2.5cm long. Its initial resistance is high (R_{ini} = 690Ω) compared to the value on glass of 250Ω. The 2D stretched sample (sample 2), 100μm wide and 5cm long, had an initial resistance of R_{init} = 3,564Ω (R~1,000Ω calculated from conductor geometry).
Sample 1 was uni-axially stretched in steps of 1% strain every 60 seconds. Its electrical resistance R_1 was recorded every 30 seconds. R_1 increases steadily by 270% to R_{max} = 2,550Ω at ε_x = 60% strain. Despite the high applied strain, the sample did not fail electrically, and negligible macroscopic change in the film was observed.

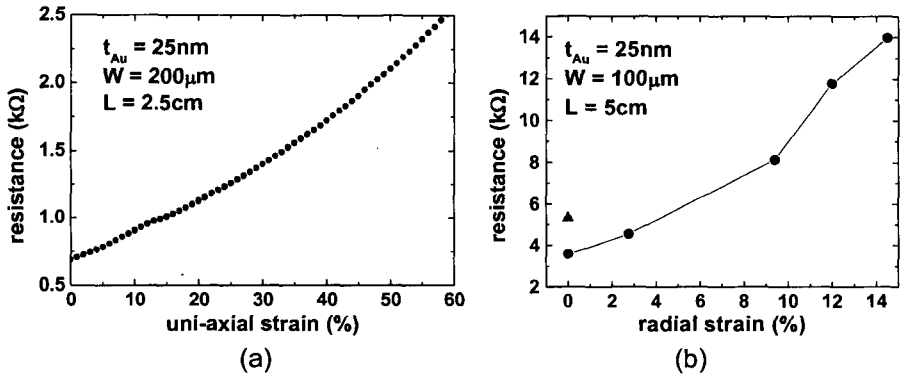

Figure 4. Electrical resistance of 25nm thick gold conductor on PDMS membrane as a function of applied tensile strain (a) Sample 1 was uni-axially stretched up to 60% strain, (b) Sample 2 was 2D radially stretched up to 14.5% radial strain; ▲ is the value after relaxation to 0% strain[19].

Sample 2 was radially stretched. It was held stretched for ~5-10min at every step. At ε_r = 14.5%, its electrical resistance R_2 had risen by ~300%. The sample did not fail electrically. After release from the biaxial stretching R_2 dropped back to 5,300Ω. $R_2(\varepsilon_r)$ was reproduced in four stretching cycles between 0% and ~8% radial strain. After fabrication and under the optical microscope all gold layers are shiny and continuous. No macroscopic change was observed in the surface of the gold film after 2D radial stretching, and no transversal cracks are visible. The Au film still has a low resistance.

4.3. *Fatigue*

We evaluated the reliability of stretchable interconnects under prolonged mechanical cycling. A 80μm wide, 1.6cm long gold interconnect on 1mm thick PDMS is mounted in the uni-axial stretching set up and cycled between 0 and 10% strain with a 0.5% step every 15s. Every cycle takes 600s.

Figure 5 shows the electrical resistance of the interconnect on PDMS under cyclic strain. The initial resistance of the conductor was 60Ω. We observed three regimes in the variation of the electrical resistance as a function of strain:

(i) during the very first cycles, the resistance changes little with the applied strain.

(ii) after 500 cycles, the maximum resistance at 10% strain has increased by 80%. The minimum value at 0% strain is ~ 65Ω.

(iii) during the last 100 cycles, the resistance has doubled at the maximum applied strain, but remains at ~60Ω at 0% strain.

The interconnect withstood 1,000 cycles without electrical failure. Improving the cycling performance of the conductors awaits a deeper understanding of the mechanism of reversible stretching.

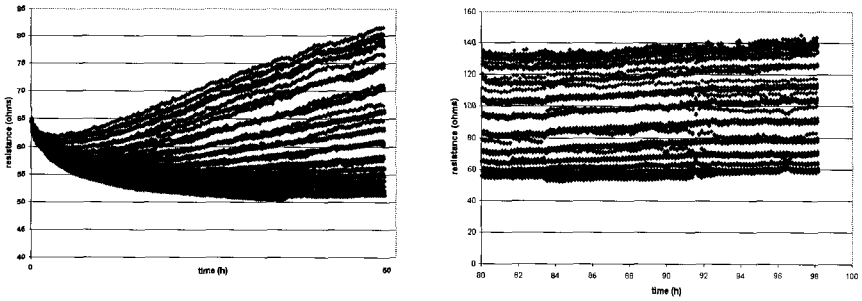

(i) 0 - 328 first cycles (iii) 680 – 1,000 cycles

Figure 5. Electrical resistance at two stages (i) and (iii) during mechanical cycling between 0% and 10% strain of a Au conductor made on PDMS. One strain cycle is 600 seconds long.

5. The first elastic circuit

We fabricated an elastic inverter circuit based on elastomeric interconnects and discrete amorphous silicon thin film transistors (a-Si:H TFT) that had been fabricated on polyimide foil substrate[20]. The circuit schematic, and a photograph of the circuit and of one TFT are shown in Figure 6. The TFTs were fabricated on 50μm thick Kapton E polyimide foil[21]. Gold pads and stretchable interconnects were patterned directly on the PDMS. Both TFTs are mounted face-down (seen through the Kapton in the small photograph) on the Au/PDMS pads. The "TFT islands" remain in place during the stretching experiments due to the tackiness of the elastomer. Off-membrane input/output contacts were prepared using the procedure described in section 4.1.

The ON resistance of the a-Si TFTs is of the order of 2MΩ. As the resistance of the interconnects lies in the range of 0.1kΩ to 1kΩ, they have a negligible effect on the overall circuit resistances.

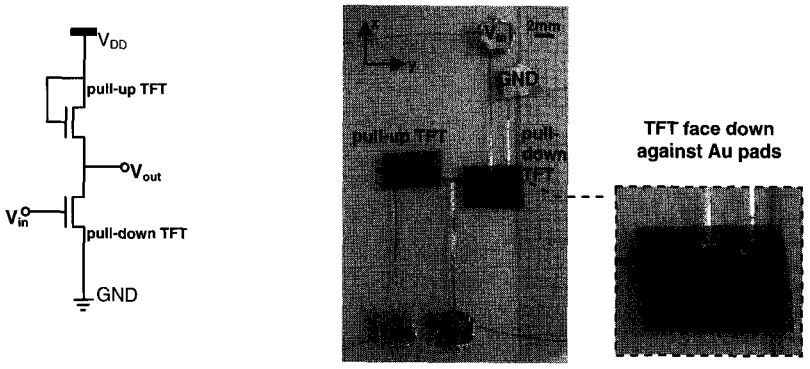

(a) (b)

Figure 6. Elastic thin-film transistor invertor. (a) Sketch of the circuit. (b) Picture of the stretchable inverter. The clear PDMS substrate covers the entire frame, and is partially underlaid by paper ruled with a millimeter scale[20]. Inset: one TFT with matching contacts mounted face-down on the gold pads on PDMS.

We evaluated the electrical and mechanical performance of the inverter in its relaxed state and stretched by up to 12%. The circuit was mounted in a manual uni-axial stretcher. It was stretched in steps of ~2.5%, held stretched for 1 minute, and released to its initial position for 5 minutes; the same sequence was repeated for 5, 7.5, 10 and 12% of elongation, so that the 40-mm long circuit was stretched by up to 12%.

Figure 7a presents the AC responses of the stretchable inverter driven with a 14V amplitude 50Hz square wave in the initial (0% strain), stretched (12% strain) and relaxed (0% strain) states. The AC response is seen to be little affected by the mechanical deformation. The circuit kept operating over the ten stretching cycles that we applied.

The DC electrical performance of the inverter was recorded prior to, during, and after uni-axial stretching by up to 10% (Figure 7b). The relaxed inverter begins to switch at $V_{IN} \sim 5V$. The circuit has a gain S of ~1.3, in agreement with a circuit model based on our TFT characteristics. The gain was low because the pull-up and pull-down TFTs are identical. At 10% tensile strain the transfer characteristic slightly drifts towards higher output voltages, reducing the circuit gain. We believe this is due to the shearing of the electrical contacts between the TFT/Au contact pads during the stretching. Improving the mechanical stability of contacts is now one of our priorities. The transfer characteristics in the relaxed state, prior to and after elongation, are identical.

Clearly this circuit is fully elastic, electrically as well as mechanically.

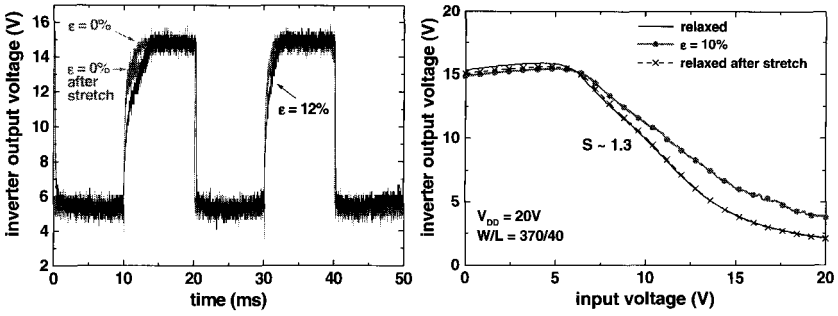

Figure 7. Electrical performance of the stretchable inverter under mechanical deformation[20]. (a) Output voltage of the inverter driven with a 14V square wave at 50Hz while relaxed prior to and after 12% stretching, and while stretched by 12%. (b) DC voltage transfer characteristics: relaxed state, prior to stretching, during, and after stretching by 10%.

6. Conclusion and perspectives

We are now able to fabricate stretchable interconnects for elastic electronic surfaces. Experiments illustrate the astonishing stretchability of thin gold conductors on PDMS membrane as well as the complex and rich nature of this new electrical component. The mechanisms of deformation and the electrical and mechanical properties of thin metal films on polymer substrates are only beginning to be understood. Substrate preparation, film growth and bonding, the built-in strain in stiff films on compliant substrates, the mechanisms of stretching, and of electrical conduction particularly across fractures, all need careful study.

Our basic theoretical result obtained so far is that certain combinations of metal and substrate indeed can be strained by up to 100% with the metal remaining continuous. This theoretical work has not yet advanced to the point of understanding the apparent elasticity of the interconnects that we observe in our experiments. We believe that the reversible stretchability derives from phenomena that occur on the nanometer scale.

But it is certain that conductors that can double their length and maintain low electrical resistance will be integrated into electronic packages and to large area and elastic circuits. Achieving fully elastic integrated circuits will require the development of novel fabrication and evaluation techniques including micro-patterning, contacting, and electrical testing.

In addition our discovery and application of stretchable interconnects on elastomeric substrates is likely to impact work with interconnects on other deformable substrates. We already have used similar metallization for interconnecting OLED pixels on domes of polyimide foil that were shaped by plastic deformation[3].

7. Acknowledgement

This research was supported by DARPA-funded AFRL-managed Macroelectronics Program Contract FA8650-04-C-7101, and by the New Jersey Commission on Science and Technology.

8. References

1. C. E. Forbes, A. Gelbman, C. Turner, H. Gleskova, and S. Wagner, Society for Information Display '02 Technical Digest Vol. 33 pp. 2000-2004, 2002.
2. G.P. Collins, Scientific American, pp. 74-81, August 2004.
3. R. Bhattacharya, S. Wagner, Y.-J. Tung, J. Esler, M. Hack, International Electron Devices, Meeting Technical Digest, pp. 15.6.1-15.6.4, 2004.
4. V.J. Lumelsky, M.S. Shur, S. Wagner, IEEE Sensor Journal, vol. 1, pp. 41-51, Jun. 2001.
5. D.W. Pashley, Proc. Roy. Soc. Lond. A, vol. 255, No. 1281, pp. 218-231, Apr. 1960.
6. P.I Hsu, M. Huang, H. Gleskova, Z. Xi, Z. Suo, S. Wagner, J.C. Sturm, IEEE Trans. Elec. Dev., vol. 51, No. 3, pp. 371-377, Jul. 2004.
7. P.I. Hsu, M. Huang, Z. Xi, S. Wagner, Z. Suo, J.C. Sturm, J. of Appl. Phys., vol. 95, No. 2, pp. 705-712, Jan. 2004.
8. S.P. Lacour, S. Wagner, Z. Huang, Z. Suo, , Appl. Phys. Lett., vol. 82, pp. 2404-2406, Apr. 2003.
9. S.P. Lacour, J. Jones, Z. Suo, S. Wagner, IEEE Elec. Dev. Lett., Vol. 25, No. 4, pp. 179-181, April 2004.
10. A.L. Volynskii, S. Bazhenov, O.V. Lebedeva, N.F. Bakeev, J. of Mat. Science, Vol. 35, pp. 547-554, 2000.
11. W.T.S. Huck, N. Bowden, P. Onck, T. Pardoen, J. Hutchinson, G.M. Whitesides, Langmuir, vol. 16, pp. 3497-3501, July 2000.
12. T. Li, Z. Huang, Z.C. Xi, S.P. Lacour, S. Wagner, Z. Suo, Mech. Mater., Vol. 37, pp. 261-273, 2005. Preprint: www.deas.harvard.edu/suo, Publication 148.
13. T. Li, Z. Huang, Z. Suo, S.P. Lacour, S. Wagner, Appl. Phys. Lett., Vol. 85, pp. 3435-3437, 2004. Preprint: www.deas.harvard.edu/suo, Publication 159.
14. T. Li, Z. Suo, "Deformability of thin metal films on elastomer substrates", *submitted*, 2005. Preprint: www.deas.harvard.edu/suo, Publication 168.
15. S.P. Lacour, J. Jones, S. Wagner, T. Li, Z. Suo, Proc. of IEEE on Flexible Electronics Technology, Vol. 93, no. 8, August 2005. *in press.*
16. W.D. Callister, Jr., Materials Science and Engineering, An Introduction, John Wiley & Sons, p. 599, 1994.
17. S.P. Lacour, S. Wagner, Z. Suo, Mat. Res. Soc. Symp. Proc., vol. 795, pp. U6.9.1-6, Dec. 2003.
18. S.P. Lacour, Z. Huang, Z. Suo, S. Wagner, Mater. Res. Soc. Proc., vol. 736, pp. D4.8.1-D4.8.6, Dec. 2002.
19. S.P. Lacour, S. Wagner, Mater. Res. Soc. Proc., vol. 854E, pp. U.12.10.1-U12.10.6, Dec. 2004.
20. S. P. Lacour, C. Tsay, S. Wagner, IEEE Electron Device Letter, Vol. 25, no. 12, pp.792-794, Dec. 2004.
21. H. Gleskova, S. Wagner, Z. Suo, Mater. Res. Soc. Proc., vol. 508, 73, 1998.